Frontiers in Health Informatics www.healthinformaticsjournal.com
ISSN-Online: 2676-7104
2024; Vol 13: Issue 4 Open Access

Nattokinase as a Cardiovascular Therapeutic Agent: Mechanistic Insights via Computational Approach

Damodar Nayak Ammunje[1*], Anbu Jayaraman[2]

[1*,2]Department of Pharmacology, Faculty of Pharmacy, M.S. Ramaiah University of Applied Sciences, M S R Nagar, Bengaluru-560054, Karnataka, India

***Corresponding author:** Damodar Nayak Ammunje
*Phone No: +91-7760634780; superdamu@gmail.com

Cite this paper as: Damodar Nayak Ammunje, Nattokinase as a Cardiovascular Therapeutic Agent: Mechanistic Insights via Computational Approach, *Frontiers in Health Informatics*, 13 (4),249-261

Abstract:
The leading global cause of death remains cardiovascular diseases (CVDs) compounded by complications such as thrombosis, hypertension, and myocardial infarction. The rising burden of CVDs further underscores the call for effective and safer treatment alternatives. Nattokinase from natto, the fermented Japanese food, shows promise in managing cardiocerebrovascular health due to its anticoagulant anti-hypertensive and circulation-enhancing properties. However, full knowledge of its mechanism of action will help optimize its therapeutic potential. This research work attempted an *in-silico* study on the models of nattokinase targeting cardiovascular disorders. The study addressed the molecular interactions of nattokinase with some vital protein targets in cardiovascular diseases using computational techniques like molecular docking and molecular dynamics simulations. Among the key receptor targets for which binding affinity was determined were β1 and β2 adrenergic receptors as well as M1 and M2 muscarinic receptors. These are integral parts of cardiophysiology – particularly in regulating heart rate responses, contractility of myocardium vasodilation processes. The findings from docking and dynamics studies provide strong binding affinities. These results offer substantial evidence that nattokinase has a promising targeted therapeutic approach for CVDs.

Key words: Nattokinase; Cardiovascular Diseases; In-Silico Approaches; Molecular Docking

Introduction:

Cardiovascular diseases (CVDs) comprise a wide range of disorders affecting the heart and blood vessels, including but not limited to coronary artery disease, cerebrovascular disease, and rheumatic heart disease. CVDs are among the leading causes of death in the world; nearly 17.9 million deaths were reported annually, representing 31% of total global mortality (https://www.who.int/news-room/fact-sheets/detail/cardiovascular-diseases). Common complications include heart failure, in which the cardiac muscle fails to pump blood properly; myocardial infarction or 'heart attack,' due to obstruction of blood flow to the heart muscle from clots or ruptured plaques; and stroke resulting from interrupted blood supply to the brain, often caused by atherosclerosis [1]. The role of CVDs as major health determinants is further emphasized by complications like arrhythmias, characterized by irregular heartbeat patterns, and peripheral artery disease, associated with reduced blood flow to extremities [2].

Risk factors for cardiovascular complications can be classified into non-modifiable and modifiable. The presence of modifiable risk factors such as hypertension, smoking, diabetes, obesity, physical inactivity, unhealthy diet patterns, and excessive alcohol consumption has an alarming increase in the prevalence of diseases [3]. On the contrary, non-modifiable risk factors that include age, gender, and family history are also significantly involved. Prevention and control require effective strategies that involve modifications in lifestyles by means of healthy dietary practices as well as regular physical activity smoking cessation and reduced consumption of alcohol [4]. Apart from that, medical interventions to include management of blood pressure, regulation of cholesterol levels; control of diabetes; screening health periodically must be performed

so as to reduce the burden CVDs. It is hoped that these focused approaches will lower the high-level impact of cardiovascular diseases on human beings and enhance general health outcomes [5].

Understanding the mechanisms of drugs, especially in polypharmacology and cardiovascular complications, is multifaceted. Traditional experimental methods, including *in vitro* and *in vivo* models, are not only labor-intensive and costly but also often fail to mimic the complexity of human physiology [6]. Moreover, as most drugs are polypharmacological with actions at multiple targets, it becomes exceedingly difficult to predict what a drug's specific mechanism of action is supposed to be [7]. Additionally, individual variation within a population due to factors such as genetic variation makes it even more difficult to determine how drugs interact with biological pathways in different groups of people [8]. The inadequacies of experimental approaches provide a case for applying modern in-silico techniques that can more efficiently and accurately gather and analyze data; simulate drug-target interactions; and predict mechanisms. These valuable computational tools can significantly supplement traditional approaches by providing critical information about the efficacy and safety of a drug [9].

Computational techniques have revolutionized the way drug mechanisms are predicted by offering inexpensive and efficient alternatives to traditional experimental approaches [10]. Molecular docking, molecular dynamics simulations, and machine learning allow researchers to investigate drug-target interactions at the molecular level, thereby providing valuable information on binding affinity, stability, and possible off-target interactions [11]. Bioinformatics tools sift through huge biological databases and determine pathways and networks affected by the drug. The methods not only speed up the drug discovery process but also increase the reliability of predictions regarding a drug's efficacy and safety, which makes them essential in any modern pharmaceutical research [12]. Computational modeling reveals new mechanisms of action for existing drugs when used in repurposing; this is particularly relevant for complex diseases like cardiovascular complications [13].

Nattokinase, a serine protease enzyme sourced from the traditional Japanese fermented food natto, has recently attracted interest for potential therapeutic applications in cardiovascular health [14]. Nattokinase is known to have fibrinolytic activity; it can dissolve fibrin clots, reduce blood viscosity, and improve circulation. This makes the enzyme a promising candidate to manage thrombotic disorders such as stroke, deep vein thrombosis, and myocardial infarction [15]. Further support for its use in hypertension management comes from its ability to degrade angiotensin-converting enzyme [16].

As a natural compound with a good safety profile and oral bioavailability, nattokinase represents an interesting option compared to synthetic anticoagulants, which are often associated with bleeding risks and require tight monitoring [14]. In-depth silico exploration of the mechanism of action of nattokinase may further elucidate its diverse effects on cardiovascular systems and hence facilitate its development as a targeted therapeutic agent.

The prediction of the mechanism of action for a drug is very important in helping to understand the therapeutic potential of a drug, its off-target effects, and also its safety and efficacy. The accurate prediction of the mechanism allows scientists to determine the molecular interactions and pathways that are modified by a drug, which in turn facilitates rational drug design and also an approach to personalized medicine [17]. This is especially important in complex conditions like cardiovascular complications where pharmacotherapy involves multiple targets as well as pathways. In addition, predictions about mechanisms can play a role in drug repurposing, wherein pre-existing drugs are identified for new therapeutic uses [18]. Computational methods constitute an essential part of this endeavor by bringing together information from biological databases, simulating interactions between drugs and targets, and predicting outcomes with great accuracy; thus in silico studies reduces dramatically the cost as well as time associated with developing new drugs [19].

The present study attempts to predict the possible mechanisms through which nattokinase, a fibrinolytic enzyme, acts in the treatment of cardiovascular complications by using in-silico methods. Cardiovascular diseases constitute one of the leading causes of mortality in the world arising from complications such as thrombosis, hypertension, and myocardial infarction; thus, there is a significant demand for effective and safe therapeutic interventions. Nattokinase has been demonstrated to possess anticoagulant, anti-hypertensive as well as circulation-enhancing properties; thus, it would be a promising candidate for treating these disorders. This study employs cap-ex computational techniques to reveal intricate mechanisms by which nattokinase operates molecular targeting pathways and potential off-target effects. Molecular docking and molecular dynamics simulations will play an instrumental role in discovering and validating probable protein targets as well as probing into binding affinities and molecular stability while predicting biological pathways downstream

of nattokinase interaction. It is justified that this will further clarify its therapeutic potential toward realizing development as a targeted treatment for cardiovascular disorders.

2. Methods

2.1 Selection and preparation of protein and ligand

Thirty-two Three-dimensional (3D) X-ray crystal structures of targets related to cardiovascular disease with less than 2.5Å was acquired from the RCSB Protein Data Bank. For the study Three -dimensional (3D) X-ray crystal structure of ligand protein with less than 2.5Å was acquired from PDB database. The proteins were subjected to pre-processing and minimized using CHARMM-GUI server. Processed files were systematically renamed and organized for further molecular docking and simulation studies [20, 21]

2.2 Protein-Protein docking

The different target proteins of cardiovascular diseases were docked with natto kinase utilizing ZDOCK server [22] (https://zdock.umassmed.edu/). It promotes global docking search on a 3D grid employing the rigid-body FFT algorithm through its user-friendly web interface that includes shape complementarity, electro statistics and statistical potential terms for scoring of the complex structures [23]. The selected protein–protein complex will be determined by the highest quantity of intermolecular hydrogen bonds, non-covalent interactions, bond distance and interacting residues formed between the proteins. The structures are visualized using Discovery Studio 3.5 [24].

2.3 Molecular dynamics simulations of docked complexes

MD simulation was done by using GROMACS software (https://www.gromacs.org/) [25, 26] binding stability of the protein complexes was assessed using CHARMM 27 force field. The MD simulation was finalized following the completion of three phases: (i) system neutralization, (ii) system energy minimization, and (iii) system equilibration. protein complexes or system was solvated using the TIP3P water model within a cubic box measuring 1.0 nanometer (nm). Sodium and chloride ions (Na+, Cl-) was introduced to balance the system for energy minimization. The steepest descent minimization algorithm was employed to establish the system's energy minimization, ensuring the maximum force remained below 1000 kJ/mol for a maximum of 50,000 steps. The system's equilibration was conducted over 50 picoseconds (ps) utilizing the Particle Mesh Ewald (PME) method for long-range electrostatics, hence enhancing the accuracy of energy estimations [27]. The complexes were maintained at a constant temperature of 300 Kelvin (K). The trajectory files of root-mean-square deviation (RMSD), root-mean-square fluctuation (RMSF), radius of gyration (Rg), and solvent accessible surface area (SASA)was analyzed to measure the binding affinity between protein complexes. Xmgrace (https://plasma-gate.weizmann.ac.il/Grace/) is utilized for visualizing RMSD, RMSF, Rg and SASA [28].

3. Results and discussion

3.1 Retrieval of ligand protein

Three -dimensional (3D) X-ray crystal structure of ligand protein with PDB Id 5GL8 with less than 2.5Å was retrieved from PDB database and was taken in to consideration for the docking the proteins were subjected to pre-processing and minimized using CHARMM-GUI server and saved for docking studies.

3.2 Molecular docking studies

Molecular docking simulations were conducted using the ZDOCK server to assess the binding potential of nattokinase against 32 target proteins associated with cardiovascular disease (CVD). The binding energies for the protein-ligand complexes were observed in the range of 2948.68 to 1312.87. Table 1 gives a detailed ZDOCK binding score presented in descending order. Out of the 32 targets, nattokinase showed remarkable binding affinity with four major proteins, which are M1 receptor, β1 receptor, β2 receptor, and M2 receptor. These receptors are crucial to the cardiovascular physiologies because they control the vasoconstriction present in the smooth muscle cells of blood vessels, increase the heart rate, enhance contractility of the myocardium, increase stroke volume, and thereby increase cardiac output. Because they are so integral to the CVD pathophysiology, they are frequently targeted therapeutically in the treatment of conditions like hypertension, angina, and heart failure. The 3D structures of top four complexes are shown in Fig 1

Table 1: Z Dock score results of the CVD targets with natto kinase

Sl. No	Target	PDB ID	Score
1	M_1 receptor	6ZFZ	2948.688
2	Beta 1	2Y03	2896.789
3	Beta 2	5D5A	2868.121
4	M_2 receptor	3UON	2825.543
5	M_3 receptor	4U15	2653.571
6	Alpha 2	6UKX	2356.105
7	Cyclooxygenase 2	5IKT	2290.783
8	Serum paraoxonase	1V04	2096.426
9	HMG CoA	1HW9	2046.254
10	CASP 9	3V3K	2028.411
11	NOS3	3EAH	1935.869
12	BAX	2LR1	1897.392
13	Renin	2V0Z	1863.433
14	NOS2	3E7G	1841.535
15	Thermolysin	5DPF	1795.248
16	CASP 3	1NME	1782.684
17	Aldosterone synthase	4ZGX	1767.711
18	TP53	1GZH	1757.542
19	ESR 1	1A52	1753.344
20	CASP 8	2K7Z	1727.186
21	MAP Kinase	4DLI	1636.284
22	MAP Kinase Latest	6QYX	1630.273
23	AKT1	7NH4	1582.504
24	ACE	1R42	1565.861
25	JUN	5T01	1547.899
26	Carbonic anhydrase II	1BN1	1532.965
27	Coagulation Factor Xa	1XKB	1518.802
28	VEGFA	6D3O	1516.453
29	Human Annexin	1B09	1506.471
30	FOS	2WT7	1483.206
31	Voltage Ca^{2+} alpha 1	3LV3	1407.816
32	L Ca^{2+} channel	2VAY	1312.87

3.3Interpretation of protein-protein interactions

Biovia discovery studio visualizer software was used to anticipate the interactions between the selected target and ligand proteins

3.3.1 Binding mode of muscarinic acetylcholine receptor(M1):

Natto kinase showed maximum binding affinity and ligand interaction with M1 receptor with a score of 2948.68 as compared to other target proteins. The natto kinase showed nine conventional hydrogen bonds and twelve carbon-hydrogen bonds with M1 receptor respectively showed in fig 1 (a) and table 2

3.3.2 Binding mode of beta-1 adrenergic receptor (β1):

Natto kinase showed ligand interaction and binding affinity with β1 receptor with a score of 2896.78. The natto kinase showed five conventional hydrogen bonds and ten carbon-hydrogen bonds and 1 Pi-Donor hydrogen bond with β1 receptor respectively showed in fig1(b) and table 2

3.3.3 Binding mode of beta-2 adrenergic receptor (β2):

Natto kinase showed ligand interaction and binding affinity with β2 receptor with a score of 2868.12. The natto kinase showed twelve conventional hydrogen bonds and ten carbon-hydrogen bonds with β2 receptor respectively showed in fig 1(c) and table 2

3.3.4 Binding mode of muscarinic acetylcholine receptor (M2):

The natto kinase showed twelve conventional hydrogen bonds and fifteen carbon-hydrogen bonds with β2 receptor respectively showed in fig1(d) and table2

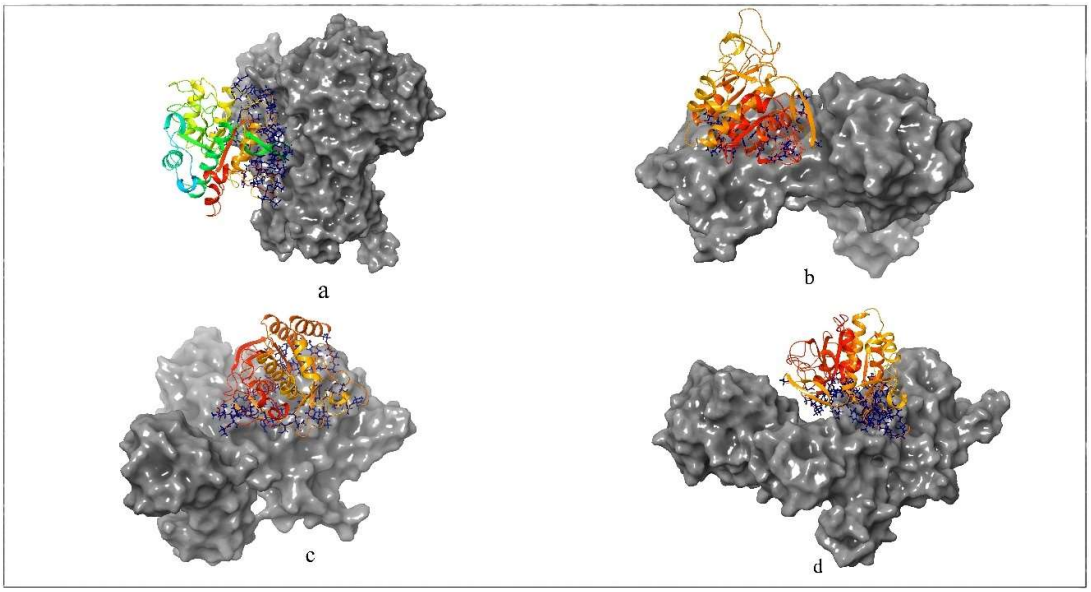

Figure 1: Representation of Nattokinase complex with **(a)** M1 receptor **(b)** beta1 receptor **(c)** M2 receptor **(d)** beta 2 receptors

Table 2: List of bonding interactions between Top four ligand protein complexes

Protein name & ID	Interacting residues		Category	Bond distance (Å)
	From	To		
M1 receptor(6ZFZ)	LYS136	ASN43	Conventional Hydrogen Bond	0.58476
	ARG141	VAL44	Conventional Hydrogen Bond	2.74205
	ALA195	SER53	Conventional Hydrogen Bond	2.58874
	ARG210	GLY211	Conventional Hydrogen Bond	2.21772
	ARG213	ALA1	Conventional Hydrogen Bond	2.73918
	ARG213	ALA1	Conventional Hydrogen Bond	2.6475
	SER63	THR202	Conventional Hydrogen Bond	1.29704
	GLY102	THR389	Conventional Hydrogen Bond	2.93644
	ASN218	LEU372	Conventional Hydrogen Bond	2.9558
	LEU156	SER49	Conventional Hydrogen Bond	2.91751
	PRO200	GLN59	Carbon Hydrogen Bond	2.36132
	THR206	TYR214	Carbon Hydrogen Bond	2.58876
	TRP209	GLN206	Carbon Hydrogen Bond	2.69255
	PRO380	ASN155	Carbon Hydrogen Bond	2.77315
	LEU386	SER101	Carbon Hydrogen Bond	2.66974
	VAL387	GLY127	Carbon Hydrogen Bond	3.07651
	PHE390	GLY102	Carbon Hydrogen Bond	2.92735
	THR55	ASN110	Carbon Hydrogen Bond	2.08355
	THR99	PHE190	Carbon Hydrogen Bond	2.34096
	SER101	THR389	Carbon Hydrogen Bond	2.12694
	GLY215	CYS205	Carbon Hydrogen Bond	2.48268
			Carbon Hydrogen Bond	
			Carbon Hydrogen Bond	
Beta-1(2Y03)	GLN70	GLU156	Conventional Hydrogen Bond	2.27996
	GLN70	SER158	Conventional Hydrogen Bond	1.4543
	GLN73	GLU156	Conventional Hydrogen Bond	2.71964
	THR164	SER62	Conventional Hydrogen Bond	2.60657
	ALA167	TYR217	Conventional Hydrogen Bond	2.77862
	ARG229	ASN117	Conventional Hydrogen Bond	2.89286
	SER188	ILE63	Conventional Hydrogen Bond	1.44008
	GLY67	SER188	Carbon Hydrogen Bond	1.62674
	SER68	SER188	Carbon Hydrogen Bond	2.87712
	ARG157	THR99	Carbon Hydrogen Bond	2.33205
	ALA170	TYR214	Carbon Hydrogen Bond	2.84922
	ILE214	SER37	Carbon Hydrogen Bond	2.56728
	ILE218	VAL44	Carbon Hydrogen Bond	2.42857
	GLY157	GLY67	Carbon Hydrogen Bond	2.40717
	SER188	ALA64	Carbon Hydrogen Bond	2.02972
	PHE189	GLY67	Carbon Hydrogen Bond	2.31066
	SER38	ILE214	Carbon Hydrogen Bond	2.54558
	ALA216	TRP166		3.3266
			Pi-Donor Hydrogen Bond	
Beta 2 (5D5A)	GLU62	GLY100	Conventional Hydrogen Bond	2.86811
	GLN65	THR99	Conventional Hydrogen Bond	2.65227
	LEU1013	SER161	Conventional Hydrogen Bond	1.84055
	LEU1015	SER194	Conventional Hydrogen Bond	2.92908
	LEU1015	GLU195	Conventional Hydrogen Bond	2.43994
	LYS1016	GLU195	Conventional Hydrogen Bond	1.6979

	LYS267	SER159	Conventional Hydrogen Bond	1.87425
	GLY102	GLU62	Conventional Hydrogen Bond	2.59811
	GLY127	GLU62	Conventional Hydrogen Bond	2.7411
	SER161	ARG1008	Conventional Hydrogen Bond	2.8821
	SER161	ILE1009	Conventional Hydrogen Bond	3.08817
	SER163	LEU1013	Conventional Hydrogen Bond	2.56113
	LYS60	THR99	Carbon Hydrogen Bond	1.96789
	ILE1009	SER161	Carbon Hydrogen Bond	3.05085
	ASP331	ASN155	Carbon Hydrogen Bond	2.2392
	CYS341	ALA216	Carbon Hydrogen Bond	1.48187
	THR99	ALA59	Carbon Hydrogen Bond	1.65492
	GLY100	LYS60	Carbon Hydrogen Bond	2.24837
	SER101	GLU62	Carbon Hydrogen Bond	2.8114
	GLU156	ASP331	Carbon Hydrogen Bond	1.5004
	SER161	ILE1009	Carbon Hydrogen Bond	2.88384
	TYR217	GLU338	Carbon Hydrogen Bond	2.61059
M2 (3U0N)	ARG211	GLY127	Conventional Hydrogen Bond	2.93945
	ARG211	GLY100	Conventional Hydrogen Bond	2.5833
	ARG211	SER125	Conventional Hydrogen Bond	0.97978
	ARG211	SER125	Conventional Hydrogen Bond	2.5006
	ARG216	ASN155	Conventional Hydrogen Bond	2.75872
	ARG216	GLU156	Conventional Hydrogen Bond	1.65233
	ALA1093	THR55	Conventional Hydrogen Bond	2.68598
	ARG1096	THR55	Conventional Hydrogen Bond	1.8787
	GLU382	SER158	Conventional Hydrogen Bond	1.93805
	ARG387	SER159	Conventional Hydrogen Bond	2.75763
	SER158	SER380	Conventional Hydrogen Bond	1.61512
	THR164	GLU382	Conventional Hydrogen Bond	2.93294
	SER210	GLY127	Carbon Hydrogen Bond	1.3436
	SER213	GLU156	Carbon Hydrogen Bond	2.43702
	PRO1086	GLY47	Carbon Hydrogen Bond	2.90319
	ASP1092	THR55	Carbon Hydrogen Bond	2.04127
	LYS1124	ASN56	Carbon Hydrogen Bond	2.3278
	LYS1124	ASN56	Carbon Hydrogen Bond	2.86446
	ARG381	SER158	Carbon Hydrogen Bond	2.84345
	ARG387	SER159	Carbon Hydrogen Bond	1.34606
	ARG387	SER159	Carbon Hydrogen Bond	2.92178
	SER49	ASP1089	Carbon Hydrogen Bond	2.49131
	THR55	LEU1091	Carbon Hydrogen Bond	2.79531
	ASN56	SER1090	Carbon Hydrogen Bond	1.89435
	ASN56	LEU1091	Carbon Hydrogen Bond	3.01086
	PRO57	ASP1089	Carbon Hydrogen Bond	1.91166
	GLY128	TYR206	Carbon Hydrogen Bond	2.51183

3.4Molecular dynamics studies

MD simulations for 100 ns were carried out for the top four Protein–Protein complexes obtained from the docking studies, that is Beta1, Beta 2, M1, M2 receptors. Trajectory analysis was performed by using GROMACS simulation package of root mean square deviation (RMSD), root mean square fluctuation (RMSF), radius of gyration (RG) and Solvent Accessible Surface Area (SASA)

RMSD is an important parameter to analyze the equilibration of MD trajectories and check the stability of complex systems during the simulation process. RMSD of the protein backbone atoms were plotted against time to assess its variations in structural conformation

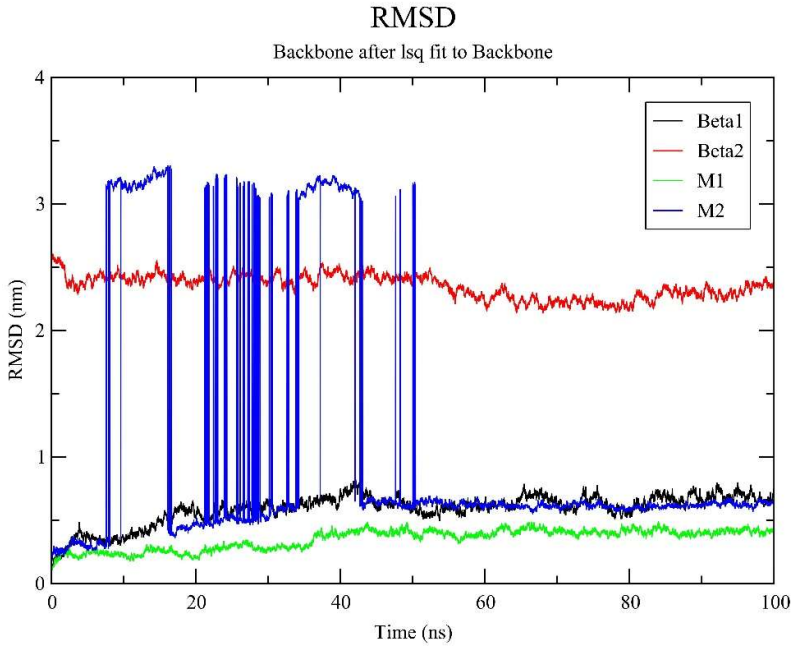

Figure 2: RMSD plot of Natto kinase with Beta1, Beta2, M1, and M2

The RMSD plot from the molecular dynamics simulation gives an idea about the structural stability of the four systems, Beta1, Beta2, M1, and M2, over a time period of 100 ns. For Beta1, represented by the black curve, there is a gradual stabilization as RMSD values remain consistently below 1 nm, which implies that this structure is stable and there is not much deviation from the initial conformation. For M1 (green curve), deviation is least; it stabilizes early in the simulation with an RMSD value around 0.5-0.6 nm indicating a rather stable structure. In contrast to this, Beta2 (red curve) shows slight conformational changes initially but then stabilizes around 2 nm and seems to be most stable at that value though some moderate changes in conformation are shown.

On the contrary, M2 (blue curve) shows exceptional fluctuation throughout the entire simulation and RMSD values shoot up repeatedly up to 3–4 nm. This is a sign of structural instability or perhaps conformational changes occurring in the system. While the other systems reach stability within the first 10–20 ns, M2 neither stabilizes nor shows any tendency to do so, which may be due to intrinsic flexibility or unresolved structural problems. The low RMSD values for M1 and Beta1 suggest that these systems remained close to their initial conformations, probably due to some good interactions or constraints. For Beta2, moderate RMSD values indicate small deviations from the starting conformation; for M2, high and fluctuating RMSD values might denote flexible loops, unstable regions, or transitions between multiple conformations.

Root Mean Square Fluctuation (RMSF) is a measure used to determine the flexibility of the residues in the molecular dynamics (MD) simulations done with GROMACS. The RMSF plot has residue number on the X-axis and fluctuation values in nanometers on the Y-axis, therefore provides information regarding the dynamic behavior of the protein or molecular system being studied. Simulations were performed for four different conditions or systems, which are labeled Beta1, Beta2, M1, and M2.

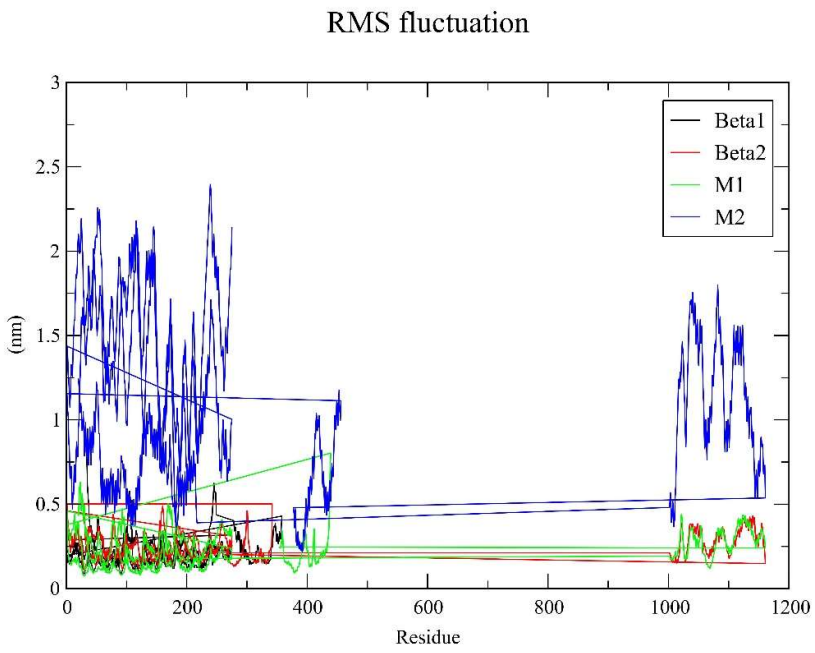

Figure 3: RMSF plot of Natto kinase with Beta1, Beta2, M1, and M2

The results show that Beta1 and Beta2, depicted by the black and red lines, respectively, show consistently low RMSF values over the entire range of residues. This indicates that the systems maintain their structural rigidity throughout the simulation. M1, represented by the green line, shows higher but somewhat stable fluctuations while M2 exhibits exceptional flexibility in certain regions with peaks of RMSF values between residues 0–200 and 1000–1200 compared to other regions. These regions are likely corresponding to loop regions or termini which are generally less compacted and more mobile. In contrast, residue values in the middle range (200–800) were low across all systems indicating that those regions might be stable secondary structural elements like alpha-helices or beta-sheets.

The Increased flexibility observed In the M2 system as Indicated by the higher RMSF values may be due to particular environmental factors, structural changes, or interactions at the molecular level that influence the dynamics of those regions. This kind of flexibility would indeed be critical in functional processes, for example, ligand binding, enzymatic activity, or conformational change. The more rigid behavior exhibited by Beta1 and Beta2 systems might result from such stabilizing interactions-higher hydrogen bonding or binding constraints, for instance-which could restrict molecular mobility in general.

The Radius of Gyration (Rg) graph is a perfect Indicator of the closeness and relative structural robustness of the molecular systems throughout the MD simulations. The X-axis in the graph corresponds to simulation time measured in nanoseconds, while the Y-axis represents the radius of gyration, noted in nanometers.

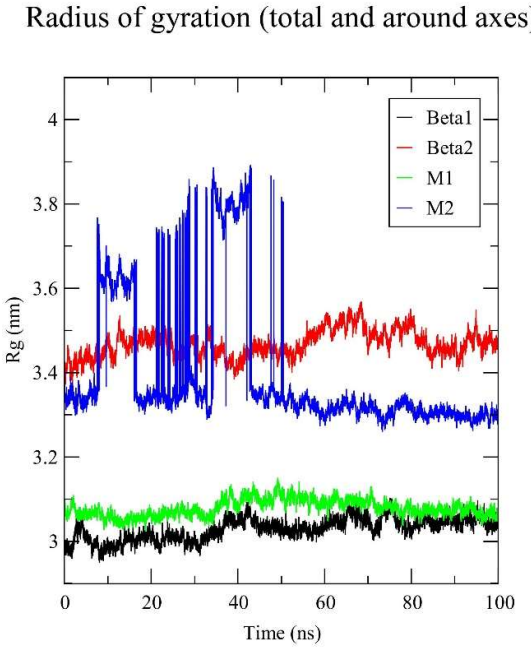

Figure 4: Radius of Gyration (Rg) of Natto kinase with Beta1, Beta2, M1, and M2

The Rg values for Beta1 (black) the average Rg is about 3.0 nm with really slight variation that would indicate a rather compact and homogeneous structure and M1(green) The green plot corresponding to gives similar Rg values, around 3.0 nm, as observed for Beta1, indicating a compact structure with rather negligible deviations. Beta2 (red) are constant during the simulation. For Beta2, the average Rg is around 3.4 nm, which denotes a system slightly less compact than the previous one but still of rather good structural stability over time.

In contrast, Rg values for M2 (blue plot) are significantly higher and average about 3.6–3.8 nm with large fluctuation rates, particularly during the initial phase of the simulation. The fluctuations would imply a more dynamic structure, possibly undergoing conformational changes or structural rearrangements during the simulation. Rg of M2 stabilizes somewhat after initial fluctuations but remains higher than that for the other systems, indicating a less compact and probably more flexible system.

The overall analysis of the Rg graph shows that the systems have different structural characteristics. Beta1, Beta2, and M1 are found to be stable and compact in contrast to M2 which is more fluctuating with higher Rg values, probably due to the influence of environmental factors, conformational changes, or ligand interactions. Such variability may imply that a grasped role either in flexibility or conformational change might be involved for M2 and its relevance.

The SASA analysis, done with GROMACS, tells how the surfaces of the molecules are exposed to the solvent throughout the simulation. The X-axis represents time during the simulation, measured in nanoseconds, and the Y-axis corresponds to SASA values, measured in square nanometers ($nm2$).

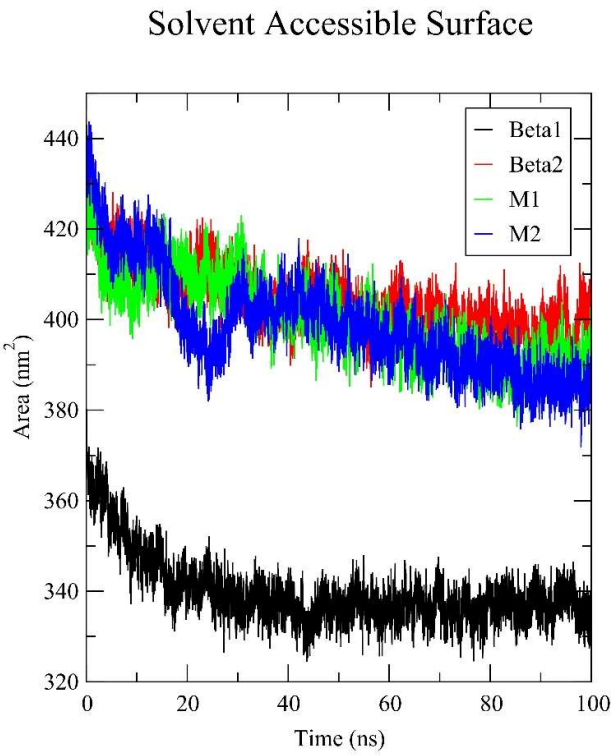

Figure 5: SASA analysis of Natto kinase with Beta1, Beta2, M1, and M2

Beta1, Beta2, M1, and M2 exhibit varying SASA values. Beta1 has the lowest average SASA values of around 340–350 $nm2$, which implies that it has a very compact structure with less access to the solvent. This indicates that Beta1 does not fluctuate much in its conformation but rather maintains a stable folded form throughout the simulation. Beta2 and M1 have moderate SASA values that oscillate around 400–420 $nm2$, indicative of a compromise between conformational rigidity and flexibility with ample solvent accessibility over time. In sharp contrast to the latter, M2 exhibited the highest SASA values ranging from 420–440 $nm2$ with huge fluctuations indicating a non-compact and more mobile structure than the others. The increased solvent exposure in M2 could be due either to its conformational freedom or partial unfolding which may expose regions that are crucial for interactions with ligands or other biomolecules. The overall profiles of SASA reveal different behaviors in terms of structures; Beta1 is the most compact while M2 shows most flexibility and solvent exposure, probably correlating with their functional roles. Such variations in SASA may reflect the functional and structural characteristics of the systems. For instance, the larger SASA in M2 may imply that regions or sites of interaction exposed to solvent are accessible, which could promote interactions with ligands or other biomolecules. In contrast, the lower SASA in Beta1 suggests a more rigid, folded structure with fewer regions accessible to solvent.

Conclusion:

This study carried out protein-protein docking analysis of 32 protein targets relating to CVD with natto kinase as the ligand. Natto kinase showed remarkable binding activity and important molecular interactions with several targets. More importantly, natto kinase had not only strong binding affinities but also stable interactions with β1, β2, M1, and M2 receptors which would possibly be therapeutic relevance by modulation of these key cardiovascular targets. further detailed assessment of MD simulation results, which includes graphs of RMSD, RMSF, Rg, and SASA, significant differences are observed in the dynamic behaviors among the four systems: Beta1, Beta2, M1, and M2.

A detailed analysis of RMSD, RMSF, Rg, and SASA reveals significant differences in the structural and dynamic behaviors of the four systems. Beta1 is the most stable and compact with less solvent exposure. Beta2 and M1 present moderate stability with more accessible solvent, showing rather balanced structural characteristics. Conversely, M2 is much more flexible with higher solvent exposure and conformational variability, which might imply its functional versatility under adaptability, such as ligand binding. Such information gives profound insight into the dynamics of structure formation in those systems studied and paves the way for further exploring their functional roles and structures.

In silico validation thus indicates that natto kinase is a probable candidate for significant inhibition of β1, β2, M1, and M2 receptors which are integral parts of the major pathways driving forward CVD. This will support the concept of natto kinase as a targeted therapeutic agent in the management of CVD; further experimental and clinical investigation is warranted to confirm its mechanism of action and therapeutic efficacy.

Acknowledgments

The authors thank the management of the M. S. Ramaiah University of Applied Sciences, Bangalore, Karnataka, India, for providing all the research facilities required.

Conflict of interest

The authors declare that they have no conflict of interest.

Consent for Publication

The authors give the consent for publication.

Data Availability

All data generated or analyzed during this study are included in this manuscript.

References:

[1] A. Barkhudaryan, W. Doehner, N. Scherbakov, Ischemic stroke and heart failure: facts and numbers. An update, Journal of clinical medicine, 10 (2021) 1146.

[2] V. Aboyans, R. Bauersachs, L. Mazzolai, M. Brodmann, J.F.R. Palomares, S. Debus, J.-P. Collet, H. Drexel, C. Espinola-Klein, B.S. Lewis, Antithrombotic therapies in aortic and peripheral arterial diseases in 2021: a consensus document from the ESC working group on aorta and peripheral vascular diseases, the ESC working group on thrombosis, and the ESC working group on cardiovascular pharmacotherapy, European Heart Journal, 42 (2021) 4013-4024.

[3] S. Li, Z. Liu, P. Joseph, B. Hu, L. Yin, L.A. Tse, S. Rangarajan, C. Wang, Y. Wang, S. Islam, Modifiable risk factors associated with cardiovascular disease and mortality in China: a PURE substudy, European Heart Journal, 43 (2022) 2852-2863.

[4] M.F. Piepoli, A.W. Hoes, S. Agewall, C. Albus, C. Brotons, A.L. Catapano, M.-T. Cooney, U. Corrà, B. Cosyns, C. Deaton, Guidelines: Editor's choice: 2016 European Guidelines on cardiovascular disease prevention in clinical practice: The Sixth Joint Task Force of the European Society of Cardiology and Other Societies on Cardiovascular Disease Prevention in Clinical Practice (constituted by representatives of 10 societies and by invited experts) Developed with the special contribution of the European Association for Cardiovascular Prevention & Rehabilitation (EACPR), European heart journal, 37 (2016) 2315.

[5] D.K. Arnett, R.S. Blumenthal, M.A. Albert, A.B. Buroker, Z.D. Goldberger, E.J. Hahn, C.D. Himmelfarb, A. Khera, D. Lloyd-Jones, J.W. McEvoy, 2019 ACC/AHA guideline on the primary prevention of cardiovascular disease: a report of the American College of Cardiology/American Heart Association Task Force on Clinical Practice Guidelines, Journal of the American College of cardiology, 74 (2019) e177-e232.

[6] A. van de Stolpe, J. den Toonder, Workshop meeting report Organs-on-Chips: human disease models, Lab on a chip, 13 (2013) 3449-3470.

[7] P. Ryszkiewicz, B. Malinowska, E. Schlicker, Polypharmacology: promises and new drugs in 2022, Pharmacological Reports, 75 (2023) 755-770.

[8] C.P.I. Schärfe, R. Tremmel, M. Schwab, O. Kohlbacher, D.S. Marks, Genetic variation in human drug-related genes, Genome medicine, 9 (2017) 1-15.

[9] A.V. Srivathsa, N.M. Sadashivappa, A.K. Hegde, S. Radha, A.R. Mahesh, D.N. Ammunje, D. Sen, P. Theivendren, S. Govindaraj, S. Kunjiappan, A review on artificial intelligence approaches and rational approaches in drug discovery, Current Pharmaceutical Design, 29 (2023) 1180-1192.
[10] X. Lin, X. Li, X. Lin, A review on applications of computational methods in drug screening and design, Molecules, 25 (2020) 1375.
[11] S. AlRawashdeh, K.H. Barakat, Applications of molecular dynamics simulations in drug discovery, Computational Drug Discovery and Design, (2023) 127-141.
[12] R. Zhang, X. Zhu, H. Bai, K. Ning, Network pharmacology databases for traditional Chinese medicine: review and assessment, Frontiers in pharmacology, 10 (2019) 123.
[13] R. Liu, L. Wei, P. Zhang, When deep learning meets causal inference: a computational framework for drug repurposing from real-world data, arXiv preprint arXiv:2007.10152, (2020).
[14] H. Chen, J. Chen, F. Zhang, Y. Li, R. Wang, Q. Zheng, X. Zhang, J. Zeng, F. Xu, Y. Lin, Effective management of atherosclerosis progress and hyperlipidemia with nattokinase: A clinical study with 1,062 participants, Frontiers in cardiovascular medicine, 9 (2022) 964977.
[15] Y. Weng, J. Yao, S. Sparks, K.Y. Wang, Nattokinase: an oral antithrombotic agent for the prevention of cardiovascular disease, International journal of molecular sciences, 18 (2017) 523.
[16] S.M. Keziah, C.S. Devi, Fibrinolytic and ACE Inhibitory Activity of Nattokinase Extracted from Bacillus subtilis VITMS 2: A Strain Isolated from Fermented Milk of Vigna unguiculata, The protein journal, 40 (2021) 876-890.
[17] M. Schirle, J.L. Jenkins, Identifying compound efficacy targets in phenotypic drug discovery, Drug discovery today, 21 (2016) 82-89.
[18] L. Chaffey, A. Roberti, D.R. Greaves, Drug repurposing in cardiovascular inflammation: Successes, failures, and future opportunities, Frontiers in Pharmacology, 13 (2022) 1046406.
[19] S. Atasever, In silico drug discovery: a machine learning-driven systematic review, Medicinal Chemistry Research, (2024) 1-26.
[20] G.K. Radhakrishna, S.H. Ramesh, S.D. Almeida, G. Sireesha, S. Ramesh, P. Theivendren, A. Kumar, K. Chidamabaram, D.N. Ammunje, S. Kunjiappan, Capsaicin-entangled Multi-walled Carbon Nanotubes against Breast cancer: A Theoretical and Experimental Approach, Journal of Cluster Science, (2024) 1-21.
[21] M. Arumugam, B. Shanmugavel, M. Sellppan, P. Pavadai, In silico evaluation of some commercially available terpenoids as spike glycoprotein of SARS-CoV-2–inhibitors using molecular dynamic approach, Journal of Biomolecular Structure and Dynamics, 42 (2024) 1072-1078.
[22] B.G. Pierce, K. Wiehe, H. Hwang, B.-H. Kim, T. Vreven, Z. Weng, ZDOCK server: interactive docking prediction of protein–protein complexes and symmetric multimers, Bioinformatics, 30 (2014) 1771-1773.
[23] R. Chen, Z. Weng, Docking unbound proteins using shape complementarity, desolvation, and electrostatics, Proteins: Structure, Function, and Bioinformatics, 47 (2002) 281-294.
[24] J.J. James, P. Pavadai, K. Sandhya, Screening of Placental Proteins Against Proteases for their Potential Use in Osteoarthritis: A Computational Approach, Current Trends in Drug Discovery, Development and Delivery (CTD4-2022), 358 (2023) 57.
[25] N.F. Rosilan, M.A.M. Jamali, S.A. Sufira, K. Waiho, H. Fazhan, N. Ismail, Y.Y. Sung, Z.-A. Mohamed-Hussein, A.A.A. Hamid, N. Afiqah-Aleng, Molecular docking and dynamics simulation studies uncover the host-pathogen protein-protein interactions in Penaeus vannamei and Vibrio parahaemolyticus, Plos one, 19 (2024) e0297759.
[26] M.J. Abraham, T. Murtola, R. Schulz, S. Páll, J.C. Smith, B. Hess, E. Lindahl, GROMACS: High performance molecular simulations through multi-level parallelism from laptops to supercomputers, SoftwareX, 1 (2015) 19-25.
[27] D. Erskine, Opacity measurements in shock-generated argon plasmas, in: AIP Conference Proceedings, American Institute of Physics, 1994, pp. 125-128.
[28] P. Turner, Center for coastal and land-margin research, Oregon Graduate Institute of Science Technology, (2005).